

Femtosecond laser-guided electric discharge in air

S. Tzortzakis,^{*} B. Prade, M. Franco, and A. Mysyrowicz[†]

Laboratoire d'Optique Appliquée, CNRS UMR 7639, Ecole Nationale Supérieure de Techniques Avancées–Ecole Polytechnique, Chemin de la Hunière, F-91761 Palaiseau Cedex, France

S. Hüller and P. Mora

Centre de Physique Théorique, CNRS UMR 7644, Ecole Polytechnique, F-91128 Palaiseau Cedex, France

(Received 11 December 2000; published 24 October 2001)

The filament due to the self-guided propagation of an infrared femtosecond laser pulse in atmospheric-pressure air is used to trigger and guide an electric discharge. The long low density plasma channel due to the filament is first heated by the Joule effect during an initial transient plasma stage. The heated channel of recombined gas then hydrodynamically expands radially. The onset of a discharge starts when the density depression on axis reaches the threshold discharge value. This model is supported by detailed experimental and numerical analysis.

DOI: 10.1103/PhysRevE.64.057401

PACS number(s): 52.80.Tn, 52.38.Hb

The initiation of an electric discharge through charged atmosphere, although complex, is basically understood. A crucial feature is the displacement of charges. Free carriers present in air gather around a point of high local field to screen it, leading to an increased local field. Eventually, the enhanced field reaches the value required to start a local avalanche process, with electrons multiplying and streaming outwards. Streamers coalesce into a self-sustained conducting path called leader. The leader moves in the direction of the opposite electrode, preceded by streamers. When contact is established, a large return current occurs. This streamer-leader interplay explains why a discharge can develop if the applied field is less than the critical field for dielectric rupture of air ($E=27$ kV/cm at atmospheric pressure). It also explains the long and erratic incubation time between application of the voltage and onset of discharge.

Several experiments have shown that laser beams can trigger electric discharges in air [1–11]. Free electrons are generated by the laser field, usually at a focal point. The same scenario as above then develops, but with a reduced incubation time for leader formation. More recently, it has been shown that the speed of leader progression can be increased considerably by focusing an intense subpicosecond laser pulse between two charged electrodes [11]. Here we report on the experimental demonstration of femtosecond filament triggered and guided electric discharge, suggesting another mechanism of laser-induced electric discharge in air. One main characteristic of this kind of discharge is that it is uniform along its axis. The basic scenario is as follows. The self-guided femtosecond infrared (IR) laser pulse, obtained as described in Ref. [12], produces in its wake a weakly ionized plasma filament with uniform longitudinal free electron density of a few times $10^{16} e^-/\text{cm}^3$ and of a length that can exceed 50 cm. This low temperature plasma filament cannot trigger by itself a self-sustained discharge between two charged electrodes during its short (ns) lifetime. On the

other hand, the current circulating during the brief conducting plasma phase produces significant Joule heating of a thin air column. This rapid heating is followed by a radial hydrodynamic expansion of the heated channel. Eventually a central air depression meets the conditions to provide a linear path for a self-discharge. This scenario is reproducible in time but occurs with a characteristic delay. We model it by taking into account the hydrodynamic expansion of the heated air into the surrounding cold air.

Figure 1 illustrates the difference between a usual [Fig. 1(a)] laser-triggered discharge and the scheme of the present experiment using a laser filament [Fig. 1(b)]. The electric circuit consists of two metallic plates (electrodes), 1.5 cm apart, with an applied voltage of 28 kV. This voltage is well below the critical field for spontaneous discharge, which is close to 40 kV [13]. Figure 1(a) shows an example of an ordinary laser-triggered discharge using a laser. Charges are deposited only at the middle point between the two electrodes by a focused femtosecond laser pulse with energy of 10 mJ. Following carrier injection by the laser, a discharge occurs with more than 90% probability. The delay between the creation of free carriers and the initiation of the discharge is long and erratic, varying typically between 1 and 5 μs . On the other hand, Fig. 1(b), which illustrates the present experiment, shows a discharge initiated and guided by a femtosecond laser-induced filament. The filament traverses and connects both electrodes through two pinholes with 3 mm diameters. It creates a uniform, partially ionized air channel that covers the whole space between the two electrodes. The onset of the discharge shown in Fig. 1(b) is now reduced to 80 ns. It occurs with 100% probability with a jitter less than 5%. The electric discharge is the result of a local on-axis air density reduction explaining on the same time the initiation and the guiding.

In order to quantify the scenario sketched above, we have performed a series of measurements to characterize the air channel at different times between the passage of the self-guided laser pulse and the onset of the discharge. These experimental results were confronted to a numerical simula-

^{*}Email address: stzortz@ensta.ensta.fr

[†]Email address: mysy@ensta.ensta.fr

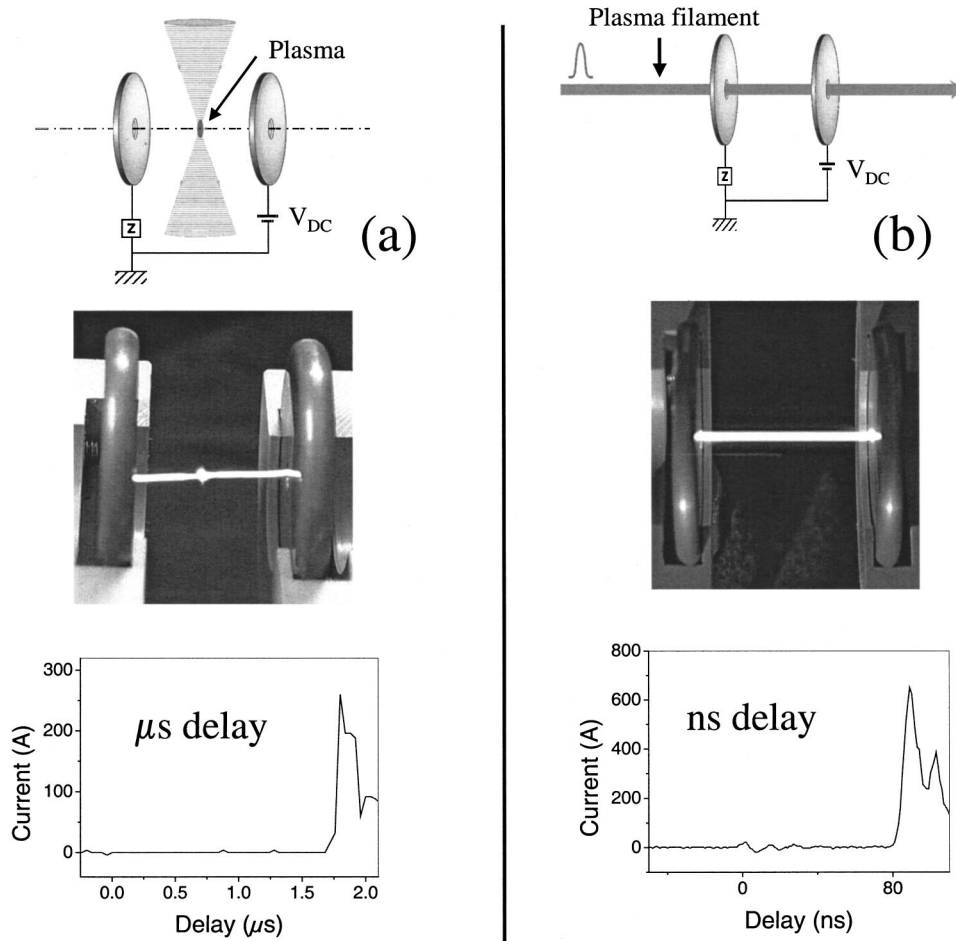


FIG. 1. Experimental configuration of the discharge circuit (a) when the laser beam is focused between the two electrodes and (b) when a self-guided filament produced plasma channel is used to connect the two electrodes. On the top of the figure is a schematic representation of the setup, while in the middle is a photo of a real experiment. At the bottom part we show characteristic curves of the current flowing in the circuit. Notice the important difference on the time delay in the two configurations.

tion. The experimental method is time-resolved diffractometry [14]. This technique allows to time resolve small local changes (gradients) of the refractive index in a gas. In a previous paper, we used this technique to characterize the initial short-lived plasma channel, its electronic density, and radial dimensions [14]. Here we measure the local changes of the refractive index of air at later times owing to the gas expansion.

The experimental setup is shown in Fig. 2. The probe beam crosses the filament path under an angle of $\theta = 4^\circ$. The probe beam was focused 3.5 cm in front of the plasma chan-

nel. A long optical delay line (from 0 to 25 m) was necessary in order to cover the whole time window between 0 and 80 ns. The spatial profile of the probe beam was cleaned after the delay line with a spatial filter in order to obtain a Gaussian profile. The far-field image of the probe beam, after crossing the heated air channel, was recorded with a linear CCD camera for different delays. Two examples of the far-field pattern observed in the presence of a direct-current field of 28 kV at 12 and 60 ns delay are shown in Fig. 2. Beam intensity profiles scanned through the fringes at different delays are shown in Fig. 3, represented by the upper curves. At

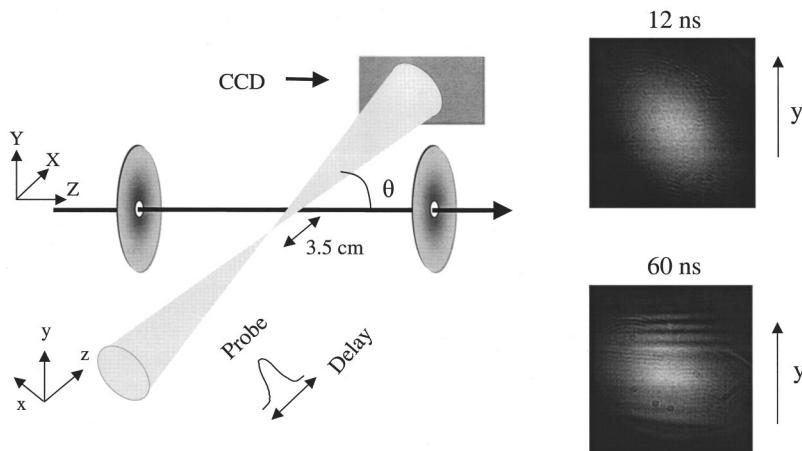


FIG. 2. Experimental configuration of the time-resolved diffractometry. The far-field images of the probe beam after crossing the heated channel are recorded for different delays. On the right two characteristic diffraction patterns at 12 and 60 ns are presented. The arrows next to the images indicate the axis along which we acquire the intensity profile that we use in our analysis (see Fig. 3).

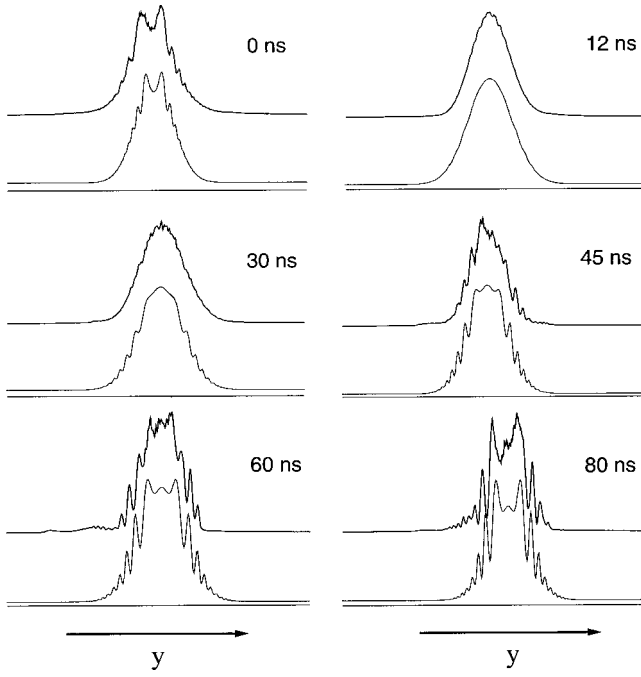


FIG. 3. Experimental results from the time-resolved diffractometry and comparison with the numerical simulations for different delays. The experimental results are represented by the upper curves while the lower ones are the simulations.

early times, just after the passage of the laser pulse [Fig. 3, (0 ns)] a dark fringe appears in the center. This is characteristic of the presence of the plasma caused by the laser pulse. It vanishes within the first nanosecond, translating the fast recombination lifetime of the electrons in the filament-generated plasma. Details on the characterization of this initial plasma and its recombination lifetime can be found in Ref. [14].

A second diffraction pattern appears after an incubation time of 30 ns [Fig. 3, (30 ns)]. The contrast of the fringes on this second diffraction pattern increases with time [Fig. 3, (45 ns, 60 ns 80 ns)] until the arrival of the discharge, after 80 ns. This second diffraction pattern occurs only in the presence of the external electric field, being a direct demonstration of its role in the Joule heating of the air channel. In the following we show that these observations are consistent with the hydrodynamic evolution of the heated air channel, creating a density depression along its axis. The expansion of the heated gas channel was computed with the hydrodynamic code MULTI [15,16]. This code has been modified appropriately for the particular conditions here. We consider cylindrical geometry to describe the radial motion around the laser axis. We also consider an ideal gas equation of state. As initial temperature perturbation we impose the radial profile:

$$T(r) = T_{room} + \delta T \exp(-r^2/w_0^2), \quad (1)$$

where δT is the temperature elevation owing to the small electric current flowing in the circuit during the first few nanoseconds and w_0 is the plasma channel waist. The following set of equations for continuity, motion, and energy are solved numerically:

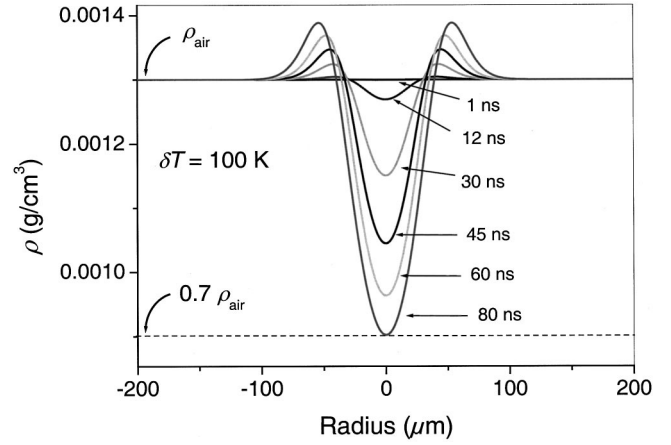


FIG. 4. Results of the hydrodynamic code MULTI for the depression of a heated channel with initial temperature elevation of 100 K and waist of 40 μm . The depression reaches the 70% limit imposed by the Paschen law (represented by the dashed line) after 80 ns in agreement with the experiment.

$$\frac{d\rho}{dt} = -\rho \vec{\nabla} \cdot \vec{u}, \quad (2)$$

$$\rho \frac{du_r}{dt} = -\frac{1}{m} \frac{\partial}{\partial r} (\rho k_B T), \quad (3)$$

$$\frac{5}{2} \frac{dT}{dt} = -T \vec{\nabla} \cdot \vec{u}, \quad (4)$$

where ρ is the gas density, \vec{u} is the velocity (retaining only the radial term of $\vec{\nabla} \cdot \vec{u}$), m stands for the mass of air molecules, and k_B is the constant of Boltzmann. Other loss terms due to collisions and radiation can be neglected.

We adopt the value of $w_0 = 40 \mu\text{m}$. This is not an adjustable parameter, but was extracted from diffraction analysis of the filament plasma channel as was reported in Ref. [14]. Thus the only adjustable parameter in our model and simulations is the initial gas temperature perturbation, which we adjust for a best fit to the experimental results. The numerical results shown in Fig. 4 correspond to an ambient temperature $T_{room} = 300 \text{ K}$ with an initial temperature increase of $\delta T = 100 \text{ K}$. An outgoing pressure wave is observed, with a central depression eventually reaching 30% of the initial value after 80 ns. This value in turn is in agreement with the threshold pressure expected for the onset of a discharge as calculated according to the Paschen law and represented by the dashed line in Fig. 4.

From the density profiles obtained from the hydrosimulations one can calculate the diffraction patterns of the probe beam owing to the changes of the refractive index induced by the expansion of the channel. We express the far field probe beam intensity as:

$$|F(\vec{q})|^2 = \left| \int \int_{-\infty}^{+\infty} f(\vec{r}, z) e^{i\varphi(\vec{r})} e^{i\vec{q} \cdot \vec{r}} dx dy \right|^2, \quad (5)$$

with the probe beam electromagnetic field written as

$$f(\vec{r}, z) = \frac{1}{1 + i(z/z_r)} \exp\left(-\frac{r^2/w^2}{1 + i(z/z_r)}\right), \quad (6)$$

where $\vec{r} = x\vec{e}_x + y\vec{e}_y$, $z_r = 1$ mm is the Rayleigh length, and $w = 20$ μm is the beam waist at the focus of the $f = 0.5$ m focusing lens. The accumulated phase is $\varphi(y) = (2\pi/\lambda \sin \theta) \int_{-\infty}^{+\infty} [n(\sqrt{\mu^2 + y^2}) - n_\infty] d\mu$, where we have introduced a change of coordinates $\mu = x \cos \theta + z \sin \theta$ (for the different systems of coordinates see Fig. 2). This phase is related to the gas density $\rho(r)$ by $n(r) = 1 + C\rho(r)$. The constant C is estimated as follows. For $r \rightarrow \infty$ and $\lambda = 800$ nm the index of refraction of the air is $n_\infty = n_{air} = 1.000275$ and its density is $\rho_\infty = \rho_{air} = 1.3 \times 10^{-3}$ g/cm³, from which $C = (n_{air} - 1)/\rho_{air} = 0.21$ cm³/g.

The evolution of the fringe pattern was calculated for different temperatures of the heated channel. An excellent

agreement was found for $\delta T = 100$ K. The corresponding set of measured (upper curves) and calculated fringe patterns (lower curves) can be seen in Fig. 3. The value of $\delta T = 100$ K is also consistent with the time delay of 80 ns shown in Fig. 4.

In conclusion we have observed a new type of reproducible laser-guided electric discharge in air. It is triggered by the expansion of a thin hot air wire produced by a self-guided IR femtosecond laser pulse. From time-resolved diffraction measurements coupled with a hydrodynamic model for the wire expansion, quantitative information on the evolution of the air wire density and temperature as well as on the discharge initiation have been extracted. This type of electric discharge may find applications when on axis uniformity is crucial.

We kindly acknowledge the expert assistance of Y.-B. André and G. Hamoniaux.

-
- [1] J. R. Greig, D. W. Koopman, R. F. Fernsler, R. E. Pechacek, I. M. Vitkovitsky, and A. W. Ali, *Phys. Rev. Lett.* **41**, 174 (1978).
- [2] G. N. Aleksandrov, V. L. Ivanov, G. D. Kadzov, V. A. Parfenov, L. N. Pakhomov, V. Yu. Petrun'kin, V. A. Podlevskii, and Yu. G. Seleznev, *Sov. Phys. Tech. Phys.* **22**, 1233 (1978).
- [3] A. A. Antipov, A. Z. Grasyuk, A. K. Zhigalkyn, L. L. Losev, and V. I. Soskov, *Sov. Phys. Tech. Phys.* **36**, 490 (1991).
- [4] M. Hijikawa, H. Tamura, H. Arishima, K. Horioka, and K. Kasuya, *Appl. Phys. Lett.* **45**, 234 (1984).
- [5] C. Honda, K. Muraoka, T. Takuma, M. Akazaki, F. Kinoshita, and O. Katahira, *Electron. Eng. (Tokyo)* **114**, 32 (1993).
- [6] E. I. Asinovskii, L. M. Vasilyak, and S. Yu. Unkovskii, *Sov. Phys. Tech. Phys.* **37**, 335 (1992).
- [7] A. A. Antipov, A. Z. Grasyuk, A. K. Zhigalkyn, L. L. Losev, and V. I. Soskov, *Sov. Phys. Tech. Phys.* **36**, 490 (1991).
- [8] X. M. Zhao, J.-C. Diels, C. Y. Wang, and J. M. Elizondo, *IEEE J. Quantum Electron.* **31**, 599 (1995).
- [9] M. Miki and A. Wada, *J. Appl. Phys.* **80**, 3208 (1996).
- [10] B. La Fontaine, F. Vidal, D. Comtois, C. Y. Chien, A. Desparois, T. W. Johnston, J.-C. Kieffer, H. P. Mercure, H. Pépin, and F. A. M. Rizk, *IEEE Trans. Plasma Sci.* **27**, 688 (1999); F. Vidal *et al.*, *ibid.* **28**, 418 (2000).
- [11] D. Comtois, C. Y. Chien, A. Desparois, F. Génin, G. Jarry, T. W. Johnston, J.-C. Kieffer, B. La Fontaine, F. Martin, R. Mawassi, H. Pépin, F. A. M. Rizk, F. Vidal, P. Couture, H. P. Mercure, C. Potvin, A. Bondiou-Clergerie, and I. Gallimberti, *Appl. Phys. Lett.* **76**, 819 (2000).
- [12] S. Tzortzakis, M. A. Franco, Y.-B. André, A. Chiron, B. Lamouroux, B. S. Prade, and A. Mysyrowicz, *Phys. Rev. E* **60**, R3505 (1999).
- [13] Due to local field effects, a spontaneous discharge can occur occasionally between the edges of the electrodes, already from an applied voltage of 30 kV.
- [14] S. Tzortzakis, B. Prade, M. Franco, and A. Mysyrowicz, *Opt. Commun.* **181**, 123 (2000).
- [15] R. Ramis, R. Schmalz, and J. Meyer-ter-Vehn, *Comput. Phys. Commun.* **49**, 475 (1988).
- [16] K. Eidmann, J. Meyer-ter-Vehn, T. Schlegel, and S. Hüller, *Phys. Rev. E* **62**, 1202 (2000).